# The Time Dimensional Measurability Aware FDE Based Analysis of Active Circuit in The Fractional Domain

**Rawid Banchuin**[1] and **Roungsan Chaisricharoen**[2]


## ABSTRACT

In this research, the analysis of the active circuit in the fractional domain has been performed by using the fractional differential equation approach where the measurability in time dimension of the derivative term has also been concerned unlike the previous work. The OTA-C filter has been adopted as the candidate active circuit due to its compactness and capability to serves as the fundamental building block of more complicated circuits. The derivative term of the fractional differential equation which includes the fractional time component parameters for obtaining such time dimensional measurability has been interpreted in Caputo sense, and the analytical solution of such an equation has been determined with the aid of Laplace transformation. With the obtained solution, the time dimensional measurability aware fractional derivative based circuit responses to various inputs have been determined, the circuit fractional time constant and other crucial time parameters have been determined and the temporal behaviour of the circuit has been analysed in the fractional domain. The loci of the pole on W-plane has been determined and the stability analysis has also been presented. Moreover, we also mathematically prove that the OTA-C filter in the fractional domain can be electronically realized with time dimensional measurability awareness by using a state of the art fractional capacitor.


**Keywords**: Active Circuit, Fractional Differential Equation, Fractional Domain, OTA-C Filter, Time Dimensional Measurability

## 1. INTRODUCTION

Fractional calculus is an extension of ordinary integer calculus and has been extensively utilized in various engineering fields including bioengineering [1], [2], control theory [3], [4], electronics [5], [6], robotics [7]-[9] and signal processing [10], [11], etc. Its related differential equation namely fractional differential equation (FDE), has also been widely used in these areas. In electrical and electronic engineering, the FDE has been used in the circuit analysis in the fractional domain as proposed in much previous research, e.g. [12]-[16] etc. However, the time dimensions of the fractional derivative terms of these works generically given by $\frac{d^x}{dt^x}$ where x stands for the order of derivative which can be non-integer, are not physically measurable due to the nature of $x$. This is because such dimension are generically given by $\sec^{-x}$.

Fortunately, the fractional time component parameter, $\sigma$, has been introduced in [17] and time dimension of the fractional derivative term incorporated by this parameter i.e. $\sigma^{x-1}\frac{d^x}{dt^x}$, become $\sec^{-1}$ which is physically measurable. This is because $\sigma$ has the dimension of sec. So, the proposed $\sigma^{x-1}\frac{d^x}{dt^x}$ is capable at handling such problematic issues imposed by $\frac{d^x}{dt^x}$ which was adopted in [12]-[16]. As a result, $\sigma^{x-1}\frac{d^x}{dt^x}$ has been used in the time dimensional measurability aware fractional domain analysis of passive circuits as proposed in [18] and [19]. Unfortunately, the similar analysis of the active circuit has never been done.

Hence, the time dimensional measurability aware analysis of the active circuit in the fractional domain has been performed in this research by using the FDE based approach. The simple OTA-C filter has been adopted as the candidate active circuit as it is often cited [15], [20]-[23], more compact than the OPAMP-RC filter adopted by [16] and also serves as the fundamental building block of more complicated active circuits as can be seen from [20]-[23]. The formerly introduced fractional time component parameter incorporated fractional derivative term has been used for deriving the FDE for taking the time dimensional measurability into account. The derivative term has been defined in Caputo sense [24], [25] due to its simplicity in finding its Laplace transformation. The analytical solution has been determined by using the Laplace-inverse Laplace transformation [26] based methodology. By using the solution of the FDE, the responses to various inputs of the circuit in the fractional domain have been derived where the sinusoidal input, arbitrary periodic input and arbitrary input in a Hilbert space have also been con-

Manuscript received on May 10, 2018 ; revised on May 3, 2019.
Final manuscript received on May 18, 2019.
[1] The author is with Graduated school of IT and Faculty of Engineering, Siam University, Bangkok, Thailand, E-mail: rawid_b@yahoo.com
[2] The author is with School of IT, Mae Fah Luang University, Chiangrai, Thailand, E-mail: roungsan.cha@mfu.ac.th

sidered. The fractional time constant [18] and other crucial time parameters of the circuit have been determined and the temporal behaviour of the circuit in the fractional domain has been analysed. The loci of the circuit pole on W-plane has been determined and the stability analysis has also been performed. Moreover, we also mathematically verify that the OTA-C filter in the fractional domain can be electronically realized with time dimensional measurability awareness by using a fractional capacitor which is a state of the art electronic device. The practical fractional capacitor based results have also been simulated.

In the subsequent section, the time dimensional measurability aware FDE of the simple OTA-C filter in the fractional domain will be formulated and solved analytically. The resulting circuit responses to different input terms will be presented in section 3. By using the obtained response, the fractional time constant and other crucial time parameters can be determined and the fractional domain temporal behavior of the circuit can be analyzed as presented in section 4. The determination of the circuit pole loci on W-plane and the fractional domain stability analysis will be shown in section 5. Moreover, the mathematical verification of the fractional capacitor based realization feasibility will be performed in section 6 where the practical fractional capacitor based simulation results will also be displayed. Finally, the conclusion will be drawn in section 7.

## 2. THE TIME DIMENSIONAL MEASURABILITY AWARE FDE OF THE OTA-C FILTER IN THE FRACTIONAL DOMAIN AND ITS ANALYTICAL SOLUTION

Consider the simple OTA-C filter of our candidate active circuit, depicted in Fig. 1. By using conventional circuit analysis, the relationship between input and output voltage can be given by

$$C\frac{d}{dt}v_o(t) = g_m(v_i(t) - v_o(t)) \quad (1)$$

where $v_i(t)$ and $v_o(t)$ stand for input and output voltage.

After some rearrangement, the following ordinary differential equation (ODE) can be obtained [15]

$$\frac{d}{dt}v_o(t) + \frac{g_m}{C}v_o(t) = \frac{g_m}{C}v_i(t) \quad (2)$$

For mathematically modelling this circuit in the fractional domain, (2) must be generalized into the FDE by simply replacing the ordinary derivative by the fractional one. Unlike [15], a fractional time component parameter has also been included for obtaining the time dimensional measurability. As a result, the time dimensional measurability aware FDE of the OTA-C filter in the fractional domain can be given by

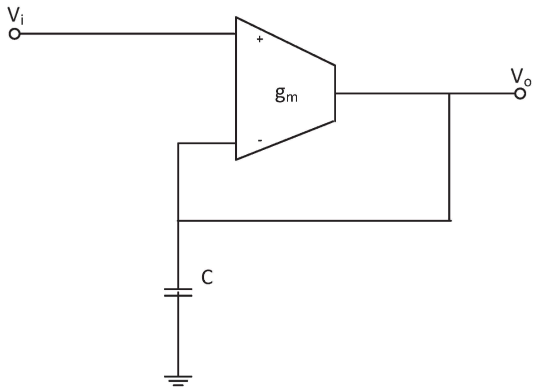


***Fig.1:*** *The simple OTA-C filter of our interested.*

$$\sigma^{\alpha-1}\frac{d^\alpha}{dt^\alpha}v_o(t) + \frac{g_m}{C}v_o(t) = \frac{g_m}{C}v_i(t) \quad (3)$$

where $\alpha$ which lies between 0 and 1, denotes the order of the fractional order derivative. Moreover, $\sigma$ is now referred to this active circuit and can be ranged from 0 to $C/g_m$. Since $\sigma$ has the dimension of sec as mentioned above, the dimension of $\sigma^{x-1}\frac{d^x}{dt^x}$, is $\sec^{-1}$ which is physically measurable. Noted that the dimentions of $\frac{d^x}{dt^x}$ is given by $\sec^{-\alpha}$ which is not physically measurable, as $\alpha$ can be fractional. It should be mentioned here that (3) will become (2) if we let $\alpha = 1$. Moreover, we define $\frac{d^x}{dt^x}$ in the Caputo sense, thus it can be mathematically defined in term of arbitrary function, $f(t)$ as [15], [24], [25]

$$\frac{d^\alpha}{dt^\alpha}f(t) = \frac{1}{\Gamma(1-\alpha)}\int_0^t \frac{f'(\tau)}{(t-\tau)^\alpha}d\tau \quad (4)$$

where $\Gamma()$ stands for the gamma function [26] and $f'(t) = \frac{d}{dt}f(t)$ [15].

In order to solve (3), the Laplace transformation must be applied to both sides of the equation. As the $\frac{d^\alpha}{dt^\alpha}$ has been defined in the Caputo sense, the Laplace transform of $\frac{d^\alpha}{dt^\alpha}v_o(t)$ can be given by [15], [24]

$$L[\frac{d^\alpha}{dt^\alpha}v_o(t)] = s^\alpha V_o(s) - s^{\alpha-1}v_o(0) \quad (5)$$

where $v_o(0)$ and $V_o(s)$ denote the initial value of output voltage and such voltage in s-domain respectively [15]. Note that $L[\frac{d^\alpha}{dt^\alpha}v_o(t)]$ can be conveniently obtained without any necessity of cumbersome fractional integration which is required if $\frac{d^\alpha}{dt^\alpha}$ has been defined by using the Riemann-Liouvielle definition [24], [25] etc. This is because we assume the Caputo definition of fractional derivative. This is the reason that this definition has been adopted in this research.

After taking the Laplace transformation, (3) become

$$\sigma^{\alpha-1}s^{\alpha}V_o(s)-\sigma^{\alpha-1}v_o(0)s^{\alpha-1}+\frac{g_m}{C}V_o(s)=\frac{g_m}{C}V_i(s) \quad (6)$$

Therefore $V_o(s)$ can be given in term of the s-domain input voltage, $V_i(s)$ as

$$V_o(s)=v_o(0)\left[\frac{s^{\alpha-1}}{s^{\alpha}+\frac{g_m}{\sigma^{\alpha-1}C}}\right]+\frac{g_m}{\sigma^{\alpha-1}C}\left[\frac{V_i(s)}{s^{\alpha}+\frac{g_m}{\sigma^{\alpha-1}C}}\right] \quad (7)$$

By using the inverse Laplace transformation and the convolution theorem [26], $v_o(t)$ can be analytically determined as follows

$$v_o(t)=v_o(0)E_{\alpha}(-\tfrac{g_m t^{\alpha}}{\sigma^{\alpha-1}C})+\tfrac{g_m}{\sigma^{\alpha-1}C}[v_i(t)*t^{\alpha-1}E_{\alpha,\alpha}(-\tfrac{g_m t^{\alpha}}{\sigma^{\alpha-1}C})] \quad (8)$$

where $*$ denotes the convolution operator. It should be mentioned here that $E_{\alpha}()$ stands for the Mittag-Leffler function [27] which can be defined in terms of an arbitrary variable $x$ as [15]

$$E_{\alpha}(x)=\sum_{k=0}^{\infty}\left[\frac{x^k}{\Gamma(\alpha k+1)}\right] \quad (9)$$

Moreover, $E_{\alpha,\alpha}()=E_{\alpha,\beta}()|_{\beta=\alpha}$ where $E_{\alpha,\beta}()$ denotes the generalized Mittag-Leffler function [26] which can be defined for any $x$ as [15]

$$E_{\alpha,\beta}(x)=\sum_{k=0}^{\infty}\left[\frac{x^k}{\Gamma(\alpha k+\beta)}\right] \quad (10)$$

It can be seen from (9) and (10) that $E_{\alpha}()=E_{\alpha,1}()$. Finally, the convolution operation can be defined for arbitrary functions $f(t)$ and $g(t)$ as follows [26]

$$f(t)*g(t)=\int_0^t f(\tau)g(t-\tau)d\tau \quad (11)$$

With this definition, (8) become

$$v_o(t)=v_o(0)E_{\alpha}(-\frac{g_m t^{\alpha}}{\sigma^{\alpha-1}C})+\frac{g_m}{\sigma^{\alpha-1}C}\int_0^t v_i(\tau)(t-\tau)^{\alpha-1}E_{\alpha,\alpha}(-\frac{g_m(t-\tau)^{\alpha}}{\sigma^{\alpha-1}C})d\tau \quad (12)$$

which is the analytical solution of (3).

By using (12), the responses of the OTA-C filter in the fractional domain to different inputs can be analytically determined as will be shown in the next section where the zero input, sinusoidal input, arbitrary periodic input and arbitrary input in a Hilbert space will be considered. It should be mentioned here that these responses and other analysis results which will be presented in the subsequent sections can serve as a basis for understanding, analysis and designing of those more complicated OTA-C filter based active circuits as any system can be well understood by first understanding of its fundamental building blocks. That is, any system with order 3 or higher can be well understood by using the understanding on the 1st and 2nd order systems as the basis, etc.

## 3. THE RESPONSE OF THE OTA-C FILTER IN THE FRACTIONAL DOMAIN TO VARIOUS INPUTS

### 3.1 Zero input

Firstly, the zero input i.e. $v_i(t)=0$, which occurs under the source free condition will be considered. By using (12), $v_o(t)$ due to such input can be simply given by

$$v_o(t)=v_o(0)E_{\alpha}(-\frac{g_m t^{\alpha}}{\sigma^{\alpha-1}C}) \quad (13)$$

and can be simulated against t by assuming that $\sigma=C/g_m$, $C=1\mu$F, $g_m=1\mu$S and $v_o(0)=1$ V. for different values of $\alpha$ given by $0.1, 0.2, 0.3, \ldots, 0.9$ as depicted in Fig. 2. It can be seen that $v_o(t)$ with larger $\alpha$ become closer to a decreasing exponential function which is the response of the OTA-C filter in the integer domain, which in turn can be modelled by using (2). This is not surprising as $E_1(x)=e^x$[27].

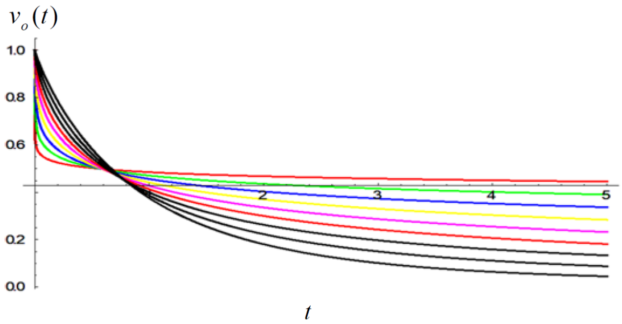


***Fig.2:*** *$v_o(t)$ (due to $v_i(t)=0$ ) v.s. t ( $\alpha$ = 0.1 (red), $\alpha$ = 0.2 (green), $\alpha$ = 0.3 (blue), $\alpha$ = 0.4 (yellow), $\alpha$ = 0.5 (pink), $\alpha$ = 0.6 (magenta), $\alpha$ = 0.7 (black), $\alpha$ = 0.8 (brown), $\alpha$ = 0.9 (gray)) .*

We have found that there exists dimensional consistency between of both sides of (13) as their dimensions are both given by V. This is because is $\frac{g_m t^{\alpha}}{\sigma^{\alpha-1}C}$ dimensionless as both $C/g_m$ and $\sigma$ has the dimension of sec.

So does $E_{\alpha}(-\frac{g_m t^{\alpha}}{\sigma^{\alpha-1}C})$ as can be seen from (9). If $\sigma$ is not included, we will have (14) which has been proposed in [15], instead. It can be seen that the dimensions of both sides of (14) are inconsistent as the

LHS has the dimension of V which contradicts that of the RHS. This is because $E_\alpha(-\frac{g_m t^\alpha}{C})$ is not dimensionless as the dimension of $\frac{g_m t^\alpha}{C}$ has been found to be $\sec^{\alpha-1}$ which is also not physically measurable.

$$v_o(t) = v_o(0)E_\alpha(-\frac{g_m t^\alpha}{C}) \tag{14}$$

## 3.2 Step input

Now $v_o(t)$ due to the step input i.e. $v_i(t) = Vu(t)$ will be formulated. By using (12), we have

$$v_o(t) = v_o(0)E_\alpha(-\frac{g_m t^\alpha}{\sigma^{\alpha-1}C}) + \frac{g_m V}{\sigma^{\alpha-1}C}\int_0^t E_{\alpha,\alpha}(-\frac{g_m(t-\tau)^\alpha}{\sigma^{\alpha-1}C})d\tau \tag{15}$$

By using (10) with $\beta = \alpha$ and the basic properties of the generalized Mittag-Leffler function [27], we have (16) from [15].

$$\int_0^t (t-\tau)^{\alpha-1}E_{\alpha,\alpha}(-\frac{g_m(t-\tau)^\alpha}{\sigma^{\alpha-1}C})d\tau = -\frac{\sigma^{\alpha-1}C}{g_m}[E_\alpha(-\frac{g_m t^\alpha}{\sigma^{\alpha-1}C}) - 1] \tag{16}$$

As a result, $v_o(t)$ can be given by

$$v_o(t) = (v_o(0) - V)E_\alpha(-\frac{g_m(t-\tau)^\alpha}{\sigma^{\alpha-1}C}) + V \tag{17}$$

If we let $v_o(0) = V$ in (17), we will have $v_o(t) = V$ which means that the DC voltage with magnitude $V$ can be obtained as the response regardless to $\alpha$. Otherwise, $v_o(t)$ can be simulated against $t$ in a similar manner to the previous subsection for different values of $\alpha$ with $V > v_o(0)$ i.e. $V = 1.5$ V. and $v_o(0) = 1$ V, as depicted in Fig. 3 which also shows that the becomes closer to the response of the integer domain filter as $\alpha$ is increased. If we let $V < v_o(0)$ by now using $V = 0.5$ V., the family of $v_o(t)$ 's can be obtained as depicted in Fig. 4.

Similarly to (13), there exists a dimensional consistency between both sides of (17) for a similar reason. Without $\sigma$, we will have (18) which has been proposed in [15] and the dimensions of both sides are inconsistent, instead.

$$v_o(t) = (v_o(0) - V)E_\alpha(-\frac{g_m(t-\tau)^\alpha}{C}) + V \tag{18}$$

## 3.3 Sinusoidal input

For the sinusoidal input i.e. $v_i(t) = V\sin(\omega t + \phi)$, $v_o(t)$ can be found by using (12) as

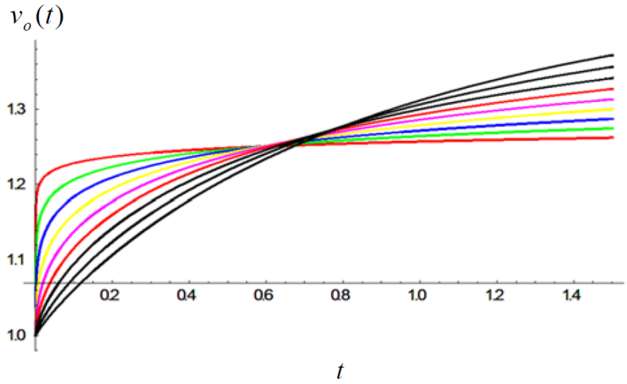


***Fig.3:*** *$v_o(t)$ (due to $v_i(t) = Vu(t)$ where $V > v_o(0)$) v.s. t ($\alpha$ = 0.1 (red), $\alpha$ = 0.2 (green), $\alpha$ = 0.3 (blue), $\alpha$ = 0.4 (yellow), $\alpha$ = 0.5 (pink), $\alpha$ = 0.6 (magenta), $\alpha$ = 0.7 (black), $\alpha$ = 0.8 (brown), $\alpha$ = 0.9 (gray)) .*

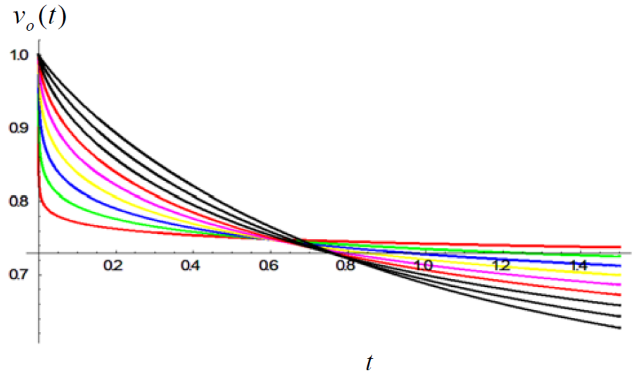


***Fig.4:*** *$v_o(t)$ (due to $v_i(t) = Vu(t)$ where $V < v_o(0)$) v.s. t ( $\alpha$ = 0.1 (red), $\alpha$ = 0.2 (green), $\alpha$ = 0.3 (blue), $\alpha$ = 0.4 (yellow), $\alpha$ = 0.5 (pink), $\alpha$ = 0.6 (magenta), $\alpha$ = 0.7 (black), $\alpha$ = 0.8 (brown), $\alpha$ = 0.9 (gray)).*

$$\begin{aligned} v_o(t) =& v_o(0)E_\alpha(-\frac{g_m t^\alpha}{\sigma^{\alpha-1}C}) \\ &+ \frac{g_m V}{\sigma^{\alpha-1}C}\int_0^t \sin(\omega\tau + \phi)(t-\tau)^{\alpha-1}E_{\alpha,\alpha}(-\frac{g_m(t-\tau)^\alpha}{\sigma^{\alpha-1}C})d\tau \end{aligned} \tag{19}$$

It can be seen that the dimensional consistency similarly to those of $v_o(t)$'s due to zero input and step input has been achieved by $v_o(t)$ due to sinusoidal input. This is because $E_\alpha(-\frac{g_m t^\alpha}{\sigma^{\alpha-1}C})$ is dimensionless and the second term on the RHS of (19) has the dimension of V as $\frac{g_m V}{\sigma^{\alpha-1}C}\int_0^t \sin(\omega\tau + \phi)(t-\tau)^{\alpha-1}E_{\alpha,\alpha}(-\frac{g_m(t-\tau)^\alpha}{\sigma^{\alpha-1}C})d\tau$ which is dimensionless. This is not surprising as the dimension of $\frac{g_m}{\sigma^{\alpha-1}C}$ is $\sec^{-\alpha}$ and that of $\int_0^t \sin(\omega\tau + \phi)(t -$

$\tau)^{\alpha-1}E_{\alpha,\alpha}(-\frac{g_m(t-\tau)^{\alpha}}{\sigma^{\alpha-1}C})d\tau$ is sec$^{\alpha}$ as both are sinusoidal and Mittag-Leffler function terms are dimensionless. Again, the obtained dimensional consistency is due to the inclusion of $\sigma$.

By using (10) with $\beta = \alpha$, (19) becomes

$$v_o(t) = v_o(0)E_{\alpha}(-\frac{g_m t^{\alpha}}{\sigma^{\alpha-1}C}) + \frac{g_m V}{\sigma^{\alpha-1}C}\int_0^t \sin(\omega\tau+\phi)(t-\tau)^{\alpha-1}\sum_{k=0}^{\infty}\left[\frac{(-\frac{g_m(t-\tau)^{\alpha}}{\sigma^{\alpha-1}C})^k}{\Gamma(\alpha k+\alpha)}\right]d\tau \quad (20)$$

After interchanging the summation and integral and performing the integration, $v_o(t)$ due to sinusoidal input can finally be given as follows

$$\begin{aligned} v_o(t) =& v_o(0)E_{\alpha}(-\frac{g_m t^{\alpha}}{\sigma^{\alpha-1}C}) \\ &- \{\sqrt{\pi}V[\omega t\cos(\phi)+2\sin(\phi)] \\ &\times\sum_{k=0}^{\infty}[(-\frac{g_m}{\sigma^{\alpha-1}C})^{k+1}2^{-\alpha(k+1)-1}t^{\alpha(k+1)} \\ &\times {}_1\tilde{F}_2(1;\frac{1}{2}(\alpha(k+1)+1),\frac{1}{2}(\alpha(k+1)+2);-\frac{1}{4}(\omega t)^2)]\} \end{aligned} \quad (21)$$

where

$$\begin{aligned} &{}_1\tilde{F}_2(1;\frac{1}{2}(\alpha(k+1)+1),\frac{1}{2}(\alpha(k+1)+2);-\frac{1}{4}(\omega t)^2) \\ &= {}_1\tilde{F}_2(a_1;b_1,b_2;z)|_{a_1=1,b_1=\frac{1}{2}(\alpha(k+1)+1),b_2=\frac{1}{2}(\alpha(k+1)+2);z=-\frac{1}{4}(\omega t)^2} \end{aligned} \quad (22)$$

It should be mentioned here that ${}_1\tilde{F}_2(;\ ,\ ;)$ is the regularized hypergeometric function with $p = 1$ and $q = 2$ [28]. The regularized hypergeometric function is briefly discussed in the appendix of the paper. If we also let $\sigma = C/g_m$, $C = 1\mu$F, $g_m = 1\mu$S and $V = 1$ V, can simulated against $t$ and $\alpha$ by assuming that $v_o(0) = 0$ V and employs $\omega = 10^6\pi$ rad/s which is obviously high, $\phi = 0$ rad and $V = 1$ V as depicted in Fig. 5 which shows that the magnitude of is inversely proportional to $\alpha$.

### 3.4 Arbitrary periodic input

According to Fourier's theorem [26], any periodic input with period T can be given as a DC term, $V_0$ plus a series of sinusoidal functions as in (23) where $V_m$ and $\phi_m$ stand for the magnitude and phase of the m$^{\text{th}}$ sinusoidal term of the series respectively. Obviously, $V_0$, $V_m$ and $\phi_m$ of them can be related to by (24)-(26) where $v_i(t)$ can be arbitrary time instant and $\omega = 2\pi/T$.

$$v_i(t) = V_0 + \sum_{m=1}^{\infty}[V_m\sin(m\omega t+\phi_m)] \quad (23)$$

$$V_0 = \frac{1}{T}\int_{\tau}^{\tau+T} v_i(t)dt \quad (24)$$

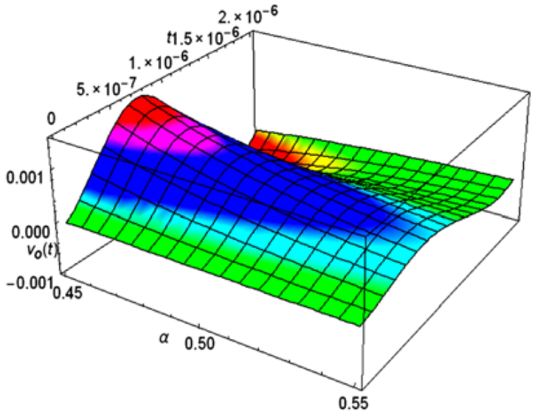


***Fig.5:*** *$v_o(t)$ due to $v_i(t) = V\sin(\omega t+\phi)$ v.s. $t$ and $\alpha$ .*

$$V_m = -\frac{2}{T}\sqrt{(\int_{\tau}^{\tau+T} v_i(t)\cos(m\omega t)dt)^2 + (\int_{\tau}^{\tau+T} v_i(t)\sin(m\omega t)dt)^2} \quad (25)$$

$$\phi_m = -\frac{\pi}{2} - \tan^{-1}\left[\frac{\int_{\tau}^{\tau+T} v_i(t)\sin(m\omega t)dt}{\int_{\tau}^{\tau+T} v_i(t)\cos(m\omega t)dt}\right] \quad (26)$$

Thus $v_o(t)$ in this case can be given by using (12) as

$$\begin{aligned} v_o(t) =& v_o(0)E_{\alpha}(-\frac{g_m t^{\alpha}}{\sigma^{\alpha-1}C}) + \frac{g_m V_0}{\sigma^{\alpha-1}C}\int_0^t (t-\tau)^{\alpha-1}E_{\alpha,\alpha}(-\frac{g_m(t-\tau)^{\alpha}}{\sigma^{\alpha-1}C})d\tau \\ &+ \frac{g_m}{\sigma^{\alpha-1}C}\int_0^t\sum_{m=1}^{\infty}[V_m\sin(m\omega\tau+\phi_m)](t-\tau)^{\alpha-1}E_{\alpha,\alpha}(-\frac{g_m(t-\tau)^{\alpha}}{\sigma^{\alpha-1}C})d\tau \end{aligned} \quad (27)$$

Since the sinusoidal term and all Mittag-Leffler function terms are dimensionless due to the effect of $\sigma$, the dimensional consistency has been achieved for $v_o(t)$. After applying (16) for evaluating the 2$^{\text{nd}}$ term of the right hand side of (27) as it is corresponded to $V_0$ which is a DC value, interchanging the summation and integral and performing the integration by using (10) with $\beta = \alpha$ for defining the generalized Mittag-Leffler function, $v_o(t)$ due to arbitrary periodic input can be finally given as follows

$$\begin{aligned} v_o(t) =& v_o(0)E_{\alpha}(-\frac{g_m t^{\alpha}}{\sigma^{\alpha-1}C}) - V_0[E_{\alpha}(-\frac{g_m t^{\alpha}}{\sigma^{\alpha-1}C})-1] \\ &- \{\sqrt{\pi}\sum_{m=1}^{\infty}\sum_{k=0}^{\infty}[[m\omega t\cos(\phi_m)+2\sin(\phi_m)]V_m \\ &\times(-\frac{g_m t^{\alpha}}{\sigma^{\alpha-1}C})^{k+1}2^{-\alpha(k+1)-1}t^{\alpha(k+1)} \\ &\times {}_1\tilde{F}_2(1;\frac{1}{2}(\alpha(k+1)+1),\frac{1}{2}(\alpha(k+1)+2);-\frac{1}{4}(\omega t)^2)]\} \end{aligned} \quad (28)$$

where

$$
\begin{aligned}
&{}_1\tilde{F}_2(1;\frac{1}{2}(\alpha(k+1)+1),\frac{1}{2}(\alpha(k+1)+2);-\frac{1}{4}(\omega t)^2) \\
&={}_1\tilde{F}_2(a_1;b_1,b_2;z)|_{a_1=1,b_1=\frac{1}{2}(\alpha(k+1)+1),b_2=\frac{1}{2}(\alpha(k+1)+2);z=-\frac{1}{4}(\omega t)^2}
\end{aligned} \tag{29}
$$

As an illustration, a sawtooth $v_i(t)$ with arbitrary period $T$ as depicted in Fig. 6 will be considered. Such $v_i(t)$ can be mathematically given for $0 \le t \le T$ by

$$v_i(t) = Vt \tag{30}$$

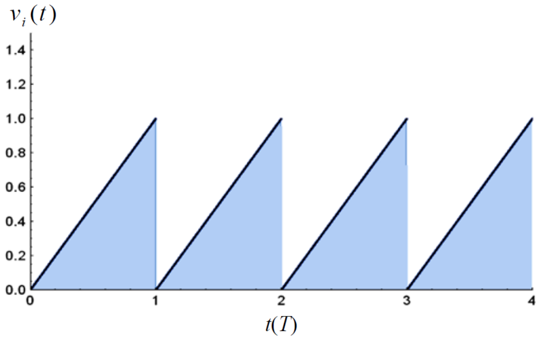


***Fig.6:*** *Sawtooth $v_i(t)$ (with arbitrary period $T$) v.s. t.*

As a result, $v_o(t)$ can be given by using (28) with the following $V_0$, $V_m$ and $\phi_m$

$$V_o = \frac{VT}{2} \tag{31}$$

$$\mathrm{V}_m = -\frac{2V}{T}\sqrt{[(\int_0^T t\cos(\tfrac{2\pi mt}{T})dt)^2 + (\int_0^T t\sin(\tfrac{2\pi mt}{T})dt)^2]} \tag{32}$$

$$\phi_m - \frac{\pi}{2} - \tan^{-1}\left(\frac{\int_0^T t\sin(\frac{2\pi mt}{T})dt}{\int_0^T t\cos(\frac{2\pi mt}{T})dt}\right) \tag{33}$$

where

$$\int_0^T t\cos(\tfrac{2\pi mt}{T})dt = t[T(\cos(\tfrac{2\pi mt}{T}) - \tfrac{mt\pi^2}{T}) + 2\pi mtSi(\tfrac{2\pi mt}{T})] \tag{34}$$

$$\int_0^T t\sin(\frac{2\pi mt}{T})dt = Tt[\sin(\frac{2\pi mt}{T}) + 2\pi Ci(\frac{2\pi mt}{T})] \tag{35}$$

Noted also that Si( ) and Ci( ) stand for sine and cosine integral function [29] respectively. Moreover, (31)-(33) can be respectively obtained by applying $v_i(t)$ as given by (30) to (24)-(26).

By also assuming a very high frequency condition for $v_i(t)$ and employing other similar assumptions to those adopted in the previous subsection, $v_o(t)$ due to sawtooth $v_i(t)$ can simulated against $t$ and $\alpha$ as depicted in Fig. 7.

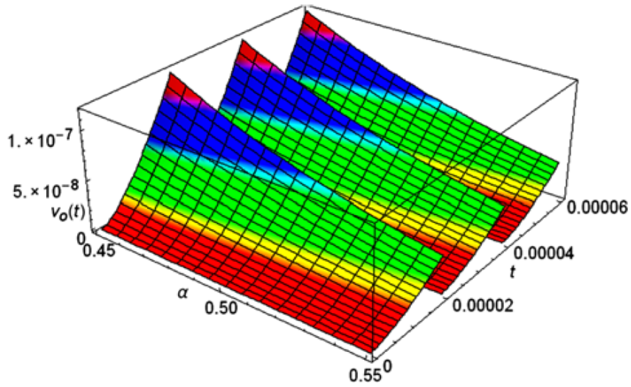


***Fig.7:*** *$v_o(t)$ (due to sawtooth $v_i(t)$) v.s. $t$ and $\alpha$.*

### 3.5 Arbitrary input in a Hilbert space

If we let $v_i(t)$ be an arbitrary element of a Hilbert space [30] with $\{v_m(t)\}$ as a basis, it can be given in a series format as follows

$$v_i(t) = \sum_{m=0}^{\infty}[\zeta_m v_m(t)] \tag{36}$$

where

$$\zeta_m = \frac{\langle v_i(t), v_m(t)\rangle}{\|v_m(t)\|^2} \tag{37}$$

Noted that $\langle,\rangle$ and $\|\ \|$ respectively denote norm and scalar product operators. By using (12), $v_o(t)$ due to such input can be obtained as given by (38) in which the dimensional consistency has been achieved. This is because the dimension of $\sum_{m=0}^{\infty}[\zeta_m \int_0^t v_m(\tau)(t-\tau)^{\alpha-1}E_{\alpha,\alpha}(-\frac{g_m(t-\tau)^\alpha}{\sigma^{\sigma\alpha-1}C})d\tau]$ is Vsec$^\alpha$ as $\zeta_m$ is dimensionless as can be seen from (37). Therefore both terms on the RHS of (38) have the dimension of V which are consistent to that of the LHS.

$$
\begin{aligned}
v_o(t) =& v_o(0)E_\alpha(-\frac{g_m t^\alpha}{\sigma^{\alpha-1}C}) \\
&+ \frac{g_m}{\sigma^{\alpha-1}C}\sum_{m=0}^{\infty}[\zeta_m \int_0^t v_m(\tau)(t-\tau)^{\alpha-1}E_{\alpha,\alpha}(-\frac{g_m(t-\tau)^\alpha}{\sigma^{\alpha-1}C})d\tau]
\end{aligned} \tag{38}
$$

## 4. THE FRACTIONAL DOMAIN TEMPORAL BEHAVIOR ANALYSIS

Before proceeding further, it should be mentioned here that such analysis to be presented in the following subsections is to study the influences of $\alpha$ to the crucial time parameters. These parameters are the fractional time constant $t_{c\alpha}$, the delay time, $t_d$, the rise time, $t_r$ and the settling time, ts, of the filter in the fractional domain where $t_{c\alpha}, t_d, t_r$ and $t_s$ will be subsequently treated.

### 4.1 The influence of $\alpha$ to $t_{c\alpha}$

Similarly to the conventional time constant of the OTA-C filter's response $t_c$, which can be given by $t_c = C/g_m$, $t_{c\alpha}$ also determines the time instant when $v_o(t)$, due to zero input given by (13), drops to approximately 36.8% of $v_o(0)$. Therefore $t_{c\alpha}$ also governs the dynamic of the OTA-C filter but in the fractional domain. By using (13) and the relationship between the fractional time constant and fractional time component parameter [18], we have found that

$$t_{c\alpha} = \frac{\sigma^{\alpha-1}C}{g_m} \tag{39}$$

which can be alternatively given by

$$t_{c\alpha} = \sigma^{\alpha-1}t_c \tag{40}$$

Obviously, it can be seen that $t_{c\alpha}$ is $\alpha$ dependent. By assuming that $t_c = 1$ sec, $t_{c\alpha}$ can be simulated against $\alpha$ as depicted in Fig. 8 which shows that $t_{c\alpha}$ is inversely proportional to $\alpha$.

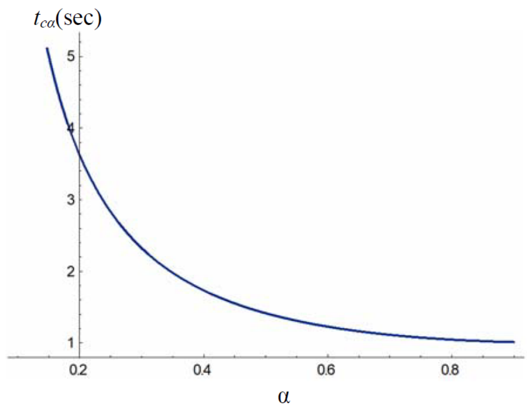


***Fig.8:*** $t_{c\alpha}$ *v.s.* $\alpha$.

### 4.2 The influence of $\alpha$ to $t_d$

Since $t_d$ can be defined as the time required for the step response to reach 10% of its steady state value, we must apply $v_o(t)$ due to step input as given by (17) for determining $t_d$. Here, we have assumed that $\lim_{t\to\infty}[v_o(t)] = 1$V. for simplicity. As a result, $t_d$ can be determined by solving

$$v_o(t_d) = 0.1 \tag{41}$$

Due to the complexity of the Mittag-Leffler function, it is convenient to solve (41) in a numerical manner where there exist various methodologies for doing so. One method is the Newton-Raphson method [26] solving for $t_d$ in an iterative manner as follows

$$t_d^{(n+1)} = t_d^{(n)} - \frac{f(t_d^{(n)})}{f'(t_d^{(n)})} \tag{42}$$

where $(n)$ means $n^{th}$ iteration of the Newton-Raphson method. Moreover, $f(t_d)$ can be given by

$$f(t_d) = v_o(t_d) - 0.1 \tag{43}$$

Thus $f'(t_d)$ can be defined as

$$f'(t_d) = \frac{d}{dt}v_o(t)\bigg|_{t=t_d} \tag{44}$$

After solving (41) with different values of $\alpha$ by assuming that $C = 1\mu$F, $g_m = 1\mu$S, $v_o(0) = 0$ V and $V = 1$ V then performing the polynomial interpolation of the results by using MATHEMATICA, $t_d$ can be simulated against $\alpha$ as depicted in Fig. 9 which shows that td is an increasing function of $\alpha$. This means that the filter in its transient state responds faster as $\alpha$ approaches 0 and becomes slower as $\alpha$ approaches 1. However, the increasing rate of $t_d$, which is low at low values of $\alpha$, becomes higher as $\alpha$ is increased toward 1. This implies that variation in the sensitivity to input of this filter at transient due to variation in $\alpha$ is low and becomes insignificant as $\alpha$ approaches 0 but gets higher as $\alpha$ approaches 1.

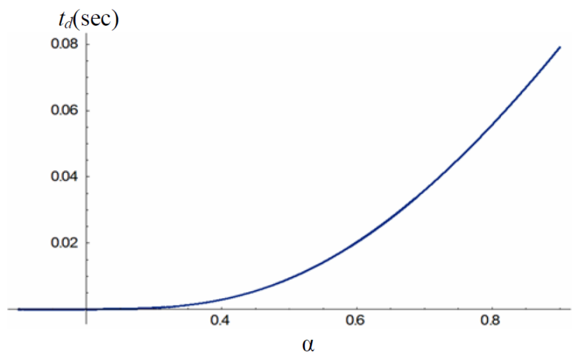


***Fig.9:*** $t_d$ *v.s.* $\alpha$.

### 4.3 The influence of $\alpha$ to $t_r$

Generally, $t_r$ can be defined as the time required for the step response to change from 10% of its steady state value to 90 %. Since we have assumed that $\lim_{t\to\infty}[v_o(t)] = 1$V, $t_r$ can be mathematically defined for this scenario as

$$t_r = t_{0.9} - t_{0.1} \tag{45}$$

where $t_{0.1}$ and $t_{0.9}$ must respectively satisfy

$$v_o(t_{0.1}) = 0.1 \tag{46}$$

$$v_o(t_{0.9}) = 0.9 \tag{47}$$

By comparing (41) and (42), we have found that $t_{0.1} = t_{0.9} - t_d$. Therefore (45) become

$$t_r = t_{0.9} - t_d \tag{48}$$

which shows that $t_r$ can be determined by first solving for t0.9 by using (47) then subtracting the obtained $t_{0.9}$ by $t_d$ as determined in the previous subsection. Note that (47) must also be solved numerically due to the complexity of the Mittag-Leffler function. After doing so for various values of $\alpha$ with other parameters similar to those assumed the previous subsection, then applying the polynomial interpolation to the obtained results, $t_r$ can be simulated against $\alpha$ as depicted in Fig. 10. Contrary to $t_d$, it can be seen from that Fig. 10 that $t_r$ is a decreasing function of $\alpha$. This means that the rate of change of $v_o(t)$ from 10% to 90% of its final value is slow as $\alpha$ approaches 0 and become faster as $\alpha$ approaches 1. It can also be seen that the decreasing rate of $t_r$ which is high as $\alpha$ approaches 0 becomes much lower as $\alpha$ is increased toward 1. This means that the variation in such rate of change caused by variation in $\alpha$ which is large as $\alpha$ approaches 0, is smaller with increasing $\alpha$ and become insignificant as $\alpha$ approaches 1.

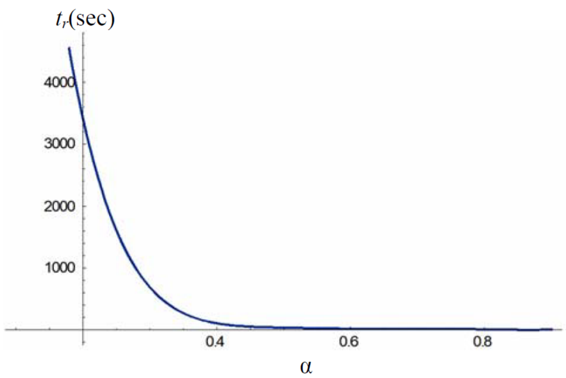


***Fig.10:*** *$t_r$ v.s. $\alpha$.*

### 4.4 The influence of $\alpha$ to $t_s$

Since $t_s$ is the time it takes for the step response to reach 98% of its final value and we have assumed that $\lim_{t\to\infty}[v_o(t)] = 1$V, such $t_s$ can be determined by solving (49) in a numerical manner for a the similar reason to those of (41) and (47).

$$v_o(t_s) = 0.98 \tag{49}$$

After doing so in a manner similar to those of the previous subsections, $t_s$ can be simulated against $\alpha$ as shown in Fig. 11. Similarly to $t_r, t_s$ is a decreasing function of $\alpha$ where the decreasing rate is large as $\alpha$ approaches 0, but becomes smaller as $\alpha$ approaches 1. This means that the filter with lower $\alpha$ settles in its steady state after that with higher $\alpha$ and vice versa. Moreover, the variation in time required for being settled of the filters when $\alpha$ approaches 0 is larger than such variation of those when $\alpha$ approaches 1.

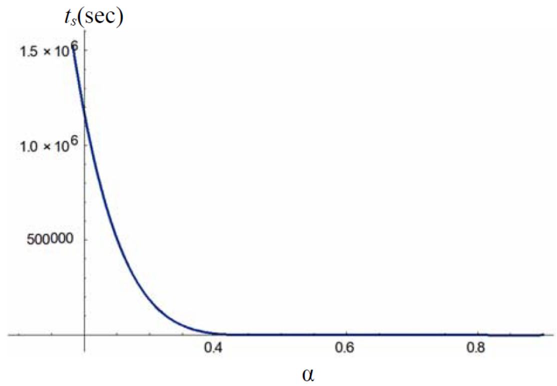


***Fig.11:*** *$t_s$ v.s. $\alpha$.*

## 5. THE POLE LOCI ON W-PLANE AND THE FRACTIONAL DOMAIN STABILITY ANALYSIS

For the stability analysis of any linear system in the fractional domain, the W-plane depicted in Fig. 12 [31], where $m$ can be arbitrary positive integer [31], must be used instead of the ordinary s-plane. From Fig. 12, it can be seen that the unstable area of W-plane is smaller than that of the s-plane which implies that the fractional domain system has a better chance of stability than that in the conventional integer domain.

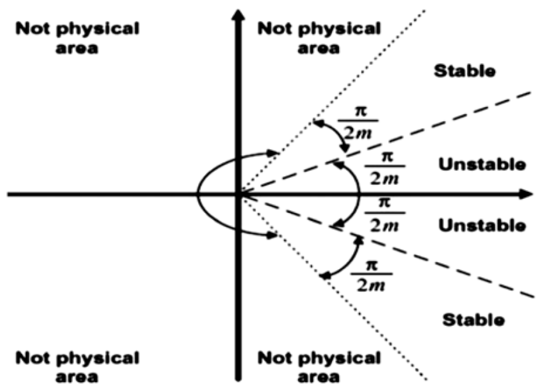


***Fig.12:*** *The W-plane [31].*

For our OTA-C filter in the fractional domain, its time dimensional measurability aware transfer function can be obtained as follows

$$H(s^\alpha) = \frac{g_m/\sigma^{\alpha-1}C}{s^\alpha + \frac{g_m}{\sigma^{\alpha-1}C}} \tag{50}$$

Thus the resulting characteristic equation has been found to be given by

$$s^{\alpha} + \frac{g_m}{\sigma^{\alpha-1}C} = 0 \tag{51}$$

For the analysis on W-plane, we let $\alpha = k/m$ and define $W$ as the rational power complex variable i.e. $\mathrm{W} = s^{1/m}$, where $k$ is a positive integer. As a result, (51) become

$$W^{k} + \frac{g_m}{\sigma^{\frac{k}{m}-1}C} = 0 \tag{52}$$

According to the criterion given by [32], we have found that all $k$ roots of (52) lie in the nonphysical region of W-plane when $\alpha < 1$, moves toward the physical region as $\alpha$ approaches 1 and will be on the boundary line of such regions when $\alpha = 1$. Since we have assumed that $\alpha$ lies between 0 and 1, these roots will never be either in the unstable region or on the marginally stable lines. So, this fractional domain active circuit is always stable without any oscillation.

## 6. THE FRACTIONAL CAPACITOR BASED REALIZATION

In [15], it has been stated that the OTA-C filter in the fractional domain can be electronically realized by simply replacing the conventional capacitor in the circuit by the state of the art fractional capacitor [33], [34]. Here, we will mathematically prove this statement and also show that the time dimensional measurability awareness can be obtained by the fractional capacitor based realization despite the fact that [15], has neglected such time dimensional measurability issue from the proposed analysis. We also display the practical fractional capacitor based simulation results. According to [35], but in the context of this work, we can define

$$C_{\alpha} = \sigma^{\alpha-1}C \tag{53}$$

where $C_{\alpha}$ stands for the pseudo capacitance of the fractional capacitor and employs the dimension of F·sec$^{\alpha-1}$ [36].

As a result, (3) become

$$\frac{d^{\alpha}}{dt^{\alpha}}v_o(t) + \frac{g_m}{C_{\alpha}}v_o(t) = \frac{g_m}{C_{\alpha}}v_i(t) \tag{54}$$

which can be converted to

$$C_{\alpha}\frac{d^{\alpha}}{dt^{\alpha}}v_o(t) = g_m(v_i(t) - v_o(t)) \tag{55}$$

Since the current-voltage relationship of such a fractional capacitor can be given by

$$i_{C_{\alpha}}(t) = C_{\alpha}\frac{d^{\alpha}}{dt^{\alpha}}v_{C_{\alpha}}(t) \tag{56}$$

where $i_{C_{\alpha}}(t)$ and $v_{C_{\alpha}}(t)$ stand for the current and voltage of the fractional capacitor, we have

$$i_o(t) = g_m(v_i(t) - v_o(t)) \tag{57}$$

after applying (56) to (55) and keeping in mind that $i_o(t)$ denotes the output current of the fractional domain OTA-C filter which flow through the fractional capacitor, thus it is equal to $i_{C_{\alpha}}(t)$.

From (56), (57) and the fact $i_o(t) = i_{C_{\alpha}}(t)$ as mentioned above, it can be seen that the OTA-C filter in the fractional domain can be electronically realized by using the fractional capacitor as previously stated in [15] where time dimensional measurability awareness can also be achieved. It should be mentioned here that such a fractional capacitor can be constructed by many means such as ferroelectric material [33], multiwall carbon nanotube (MWCNT)-epoxy nano composite material [34], RC circuit based emulation in the integer domain [37], [38] and active device based emulation [5], etc. Finally, after solving (49), we have

$$\begin{aligned} v_o(t) =& v_o(0)E_{\alpha}(-\frac{g_m t^{\alpha}}{C_{\alpha}}) \\ &+ \frac{g_m}{C_{\alpha}}\int_0^t v_i(\tau)(t-\tau)^{\alpha-1}E_{\alpha,\alpha}(-\frac{g_m(t-\tau)^{\alpha}}{C_{\alpha}})d\tau \end{aligned} \tag{58}$$

which achieves the dimensional consistency as both terms on the RHS have the dimension of V. This is because both Mittag-Leffler function terms are dimensionless and the dimension of $\frac{g_m}{C_{\alpha}}$ can be given by sec$^{-\alpha}$ due to the dimension of $C_{\alpha}$. Therefore it can be seen that the dimensional consistency can also be obtained by the fractional capacitor based realization apart from the time dimensional measurability awareness.

If we let the fractional capacitor based OTA-C filter be subjected to the DC input which can be mathematically defined in terms of step a function as $v_i(t) = Vu(t)$, the following response can be obtained

$$v_o(t) = (v_o(0) - V)E_{\alpha}(-\frac{g_m t^{\alpha}}{C_{\alpha}}) + V \tag{59}$$

By assuming that $V = 1$ V and $v_o(0) = 0$ V, $v_o(t)$'s can be simulated as depicted in Fig. 13 where the practical fractional capacitors with 3 different thicknesses of polymethyl methacrylate (PMMA) coating film on the electrode, $t_{PMMA}$ i.e. $t_{PMMA} = 3$ $\mu$m, $t_{PMMA} = 4$ $\mu$m and $t_{PMMA} = 6$ $\mu$m, [39] have been assumed. As a result, $v_o(t)$'s with different characteristics can be observed where it has been found that the magnitude of is inversely proportional to $t_{PMMA}$. Noted that $C_{\alpha}$ of these practical fractional capacitors are 419.6 F·sec$^{\alpha-1}$, 468.9 F·sec$^{\alpha-1}$ and 616.7 F·sec$^{\alpha-1}$. On the other hand, $\alpha$ are respectively 0.09, 0.11 and 0.12 [39].

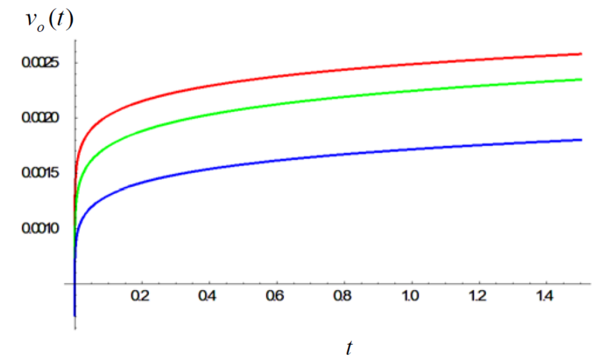


***Fig.13:*** *$v_o(t)$ due to DC input of the OTA-C filter with practical fractional capacitor with $t_{PMMA} = 3$ μm (red), $t_{PMMA} = 4$ μm (green) and $t^{PMMA} = 6$ μm (blue).*

## 7. CONCLUSION

The analysis of the active circuit in a fractional domain has been performed in this research based on an FDE approach where the time dimensional measurability of the fractional derivative term has been taken into account. The simple OTA-C filter has been adopted as the candidate circuit due to its compactness and capability to serves as the fundamental building block of more complicated circuits. The fractional time component parameter incorporated derivative term in the formulated FDE has been interpreted in the Caputo sense and the analytical solution has been determined via the Laplace transformation. By using such solution, the fractional domain dimensional consistency aware circuit responses to various inputs have been determined where the sinusoidal input, arbitrary periodic input and arbitrary input in a Hilbert space have also been considered. It should be mentioned here that those responses proposed in other time dimensional measurability studies ignored previous work as stated above, apart from [15]. They do not have dimensional consistency awareness. This is because they also lack the corresponding fractional time component parameters. The crucial time parameters i.e. $t_{c\alpha}, t_d, t_r$ and $t_s$, have been determined and the temporal behavior analysis of the circuit in a fractional domain has been performed. Moreover, the pole loci on the W-plane have been determined and the stability analysis has also been conducted. Finally, we have mathematically verified that the OTA-C filter in the fractional domain can be electronically realized with time dimensional measurability awareness and dimensional consistency by using fractional capacitor where the practical fractional capacitor based simulation results have also been shown. The OTA-C filter serves as the fundamental building block of more complicated circuits proposed analysis results as mentioned above. A good understanding of such more complicated circuits in the fractional domain can be achieved based on our analysis results. Therefore this research has been found to be beneficial to the fractional domain based analysis and design of circuits and systems.

## ACKNOWLEDGEMENT

The 1$^{st}$ author would like to acknowledge Mahidol University, Thailand for online database service.

### References

[1] R. L. Magin and M. Ovadia, "Modeling The Cardiac Tissue Electrode Interface Using Fractional Calculus," *Journal of Vibration and Control*, Vol. 14, No. 9-10, pp. 1431-1442, 2008.

[2] L.Sommacal, P.Melchior, A. Oustaloup, J.-M. Cabelguen, and A. J. Ijspeert, "Fractional Multi-Models of The Frog Gastrocnemius Muscle," *Journal of Vibration and Control*, Vol. 14, No. 9-10, pp. 1415-1430, 2008.

[3] G.W. Bohannan, "Analog Fractional Order Controller in Temperature and Motor Control Applications," *Journal of Vibration and Control*, Vol. 14, No. 9-10, pp. 1487-1498, 2008.

[4] J. Cervera and A. Bnos, "Automatic Loop Shaping in QFT Using CRONE Structures," *Journal of Vibration and Control*, Vol. 14, No. 9-10, pp. 1513-1529, 2008.

[5] B. T. Krishna and K. V. V. S. Reddy, "Active and Passive Realization of Fractance Device of Order 1/2," *Active and Passive Electronic Components*, Vol. 2008, pp. 1-5, 2008.

[6] Y. Pu, X. Yuan, K. Liao, et al., "A Recursive Two-circuits Series Analog Fractance Circuit For Any Order Fractional Calculus," *Proceedings of SPIE ICO20 Optical Information Processing*, pp. 509-519, 2006.

[7] M. F. M. Lima, J. A. T. Machado, and M. Criśostomo, "Experimental Signal Analysis of Robot Impacts in A Fractional Calculus Perspective," *Journal of Advanced Computational Intelligence and Intelligent Informatics*, Vol. 11, No. 9, pp. 1079-1085, 2007.

[8] J. Rosario, D. Dumur, and J. T. Machado, "Analysis of Fractional-order Robot Axis Dynamics," *IFAC Proceedings*, Vol. 39, No. 11, pp. 367-372, 2006.

[9] L. Debnath, "Recent Applications of Fractional Calculus to Science and Engineering," *International Journal of Mathematics and Mathematical Sciences*, Vol. 2003, No. 54, pp. 3413-3442, 2003.

[10] R. Panda and M. Dash, "Fractional Generalized Splines and Signal Processing," *Signal Processing*, Vol. 86, No. 9, pp. 2340-2350, 2006.

[11] Z.-Z. Yang and J.-L. Zhou, "An Improved Design for The IIR-type Digital Fractional Order Differential Filter," *Proceedings of the International Seminar on Future BioMedical Information Engineering (FBIE '08)*, pp. 473-476, 2008.

[12] A. A. Rousan, N. Y. Ayoub, F. Y. Alzoubi et al., "A Fractional LC?RC Circuit," *Fractional Calculus & Applied Analysis*, Vol. 9, No. 1, pp. 33-41, 2006.

[13] M. Guia, F. Gomez, and J. Rosales, "Analysis on The Time and Frequency Domain for The RC Electric Circuit of Fractional Order," *Central European Journal of Physics*, Vol. 11, No. 10, pp. 1366-1371, 2013.

[14] P. V. Shah, A. D. Patel, I. A. Salehbhai, and A. K. Shukla, "Analytic Solution for the Electric Circuit Model in Fractional Order," Abstract and Applied Analysis, Vol. 2014, pp. 1-5, 2014.

[15] R. Banchuin and R. Chaisricharoen, "Time Domain FDE Based Analysis of Active Fractional Circuit," *Proceedings of the 2018 International Conference on Digital Arts, Media and Technology (ICDAMT 2018)*, pp. 25-28, 2018.

[16] R. Banchuin and R. Chaisricharoen, "The analysis of active circuit in fractional domain," *Proceedings of the 2018 ECTI Northern Section Conference on Electrical Electronics, Computer and Telecommunications Engineering (ECTI-NCON 2018)*, pp. 25-28, 2018.

[17] J.F. Gómez-Aguilar, J.J. Rosales-García, J.J. Bernal-Alvarado, T. Córdova-Fraga and R. Guzmán-Cabrera, "Fractional Mechanical Oscillators," *Revista Mexicana de Física*, vol. 58, No. 8, pp. 348-352, 2012.

[18] G.-A. J. Francisco, R.-G. Juan, G.-C. Manuel and R.-H. J. Roberto, "Fractional RC and LC Electrical Crcuits," *Ingeniería, Investigación y Tecnología*, vol. 15, No. 2, , pp. 311-319, 2014.

[19] F. Gómez, J. Rosales and M. Gua, "RLC Electrical Circuit of Non-integer Order," *Central European Journal of Physics*, Vol.11, No. 10, pp 1361-1365.

[20] T. Deliyannis, Y. Sun, and J.K. Fidler, *Continuous - Time Active Filter Design*, CRC Press, Florida, 1999.

[21] M. Hasan and Y. Sun, "Oscillation-Based Test Structure and Method for OTA-C Filters," *Proceedings of the 13$^{th}$ IEEE International Conference on Electronics, Circuits and Systems (ICECS'06)*, pp. 98-101, 2006.

[22] D. Csipkes, G. Csipke, P. Farago, H. Fernandez-Canqueand and S. Hintea, "An OTA-C field programmable analog array for multi-mode filtering applications," *Proceedings of the 13$^{th}$ International Conference on Optimization of Electrical and Electronic Equipment (OPTIM'12)*, pp. 1176-1182, 2012

[23] P.V. Anada Mohan, *VLSI analog filters: Active RC, OTA-C and SC*, Springer, Newyork, 2013.

[24] I. Podlubny, *Fractional Differential Equations, Vol. 198 of Mathematics in Science and Engineering*, Academic Press, New York, 1999.

[25] A. Atangana and A. Secer, "A Note on Fractional Order Derivatives and Table of Fractional Derivatives of Some Special Functions," *Abstract and Applied Analysis*, Vol. 2013, pp. 1-8, 2013.

[26] E. Kreyszig, *Advanced Engineering Mathematics*, John Wiley and Sons, Inc., New York, 1999.

[27] A. M. Mathai and H. J. Haubold, *Special Functions for Applied Scientists*, Springer, New York, 2010.

[28] E. W. Weisstein, "Regularized Hypergeometric Function," *MathWorld-A Wolfram Web Resource.*

[29] M. Abramowitz and I.A. Stegun, *Handbook of Mathematical Functions with Formulas, Graphs, and Mathematical Tables*, Dover, New York, 1972.

[30] E. Ziedler, *Applied Functional Analysis*, Springer, New York, 1995.

[31] M.S. Semary, A.G. Radwan and H.N. Hassan, "Fundamentals of Fractional-order LTI Circuits and Systems: Number of Poles, Stability, Time and Frequency Responses," *International Journal of Circuit Theory and Applications*, Vol. 44, No. 12, pp. 2114-2133, 2016.

[32] A.G. Radwan, A.M. Soliman, A.S. Elwakil and A. Sedeek, "On The Stability of Linear Systems with Fractional Order Elements," Chaos, Solitons and Fractals, Vol. 40, No 5. pp. 2317-2328, 2009.

[33] A. Agambayev, S. Patole, M. Farhat, A. Elwakil, H. Bagci and K. N. Salama, "Ferroelectric Fractional-Order Capacitors," *ChemElectroChem*, Vol. 4, No. 11, pp. 2807-2813, 2017.

[34] D. A. John, S. Banerjee, G. W. Bohannan and K. Biswas, "Solid-state Fractional Capacitor Using MWCNT-epoxy Nanocomposite," *Applied Physics Letters*, Vol. 110, No. 16, pp. 163504-1-163504-5, 2017.

[35] R. Banchuin, "Novel Expressions for Time Domain Responses of Fractance Device," *Cogent Engineering*, Vol. 4, No. 1, pp. 1-28, 2017.

[36] T. J. Freeborn, B, Maundy and A.S. Elwakil, "Measurement of Supercapacitor Fractional-order Model Parameters From Voltage-excited Step Response," *IEEE Journal on Emerging and Selected Topics in Circuits and Systems*, Vol. 3, No. 3, pp. 367-376, 2013.

[37] C. Halijak, "An RC Impedance Approximant to (1/s)1/2," *IEEE Transactions on Circuit Theory*, Vol. 11, No. 4, pp. 494-495, 1964.

[38] J. Valsa and J. Vlach, "RC Models of A Constant Phase Element," *International Journal of Circuit Theory and Applications*, Vol. 41, No. 1, pp. 59-67, 2013.

[39] S. Das, K. Biswas and B. Goswami, "Study of The Parameters of A Fractional Order Capacitor," *Proceedings of INDICON 2015 Annual IEEE India Conference*, pp. 1-5, 2015.

[40] B. Dwork, *Generalized Hypergeometric Functions*, Clarendon Press, Oxford,1990.

# APPENDIX

## The regularized hypergeometric function

Let $p$ and $q$ be arbitrary positive integers, the regularized hypergeometric function with any p and q can be defined as follows [28]

$$ {}_p\tilde{F}_q(a_1, a_2, \ldots\ a_p; b_1, b_2, \ldots\ b_q; z) = \frac{{}_pF_q(a_1, a_2, \ldots, a_p; b_1, b_2, \ldots, b_q; z)}{\Gamma(b_1)\Gamma(b_2)\ldots\Gamma(b_q)} \quad (A1) $$

where ${}_pF_q(;\ ,\ ;)$ denotes the generalized hypergeometric function with arbitrary $p$ and $q$. The ${}_pF_q(;\ ,\ ;)$ can be defined as a series which converges if and only if $p \leq q$ as [39]

$$ {}_pF_q(a_1, a_2\ \ldots, a_p; b_1, b_2, \ldots\ b_q; z) = \sum_{n=0}^{\infty} \left[ \frac{\prod_{i=1}^{p} (a_i)_n}{\prod_{j=1}^{q} (b_i)_n} \frac{z^n}{n!} \right] \quad (A2) $$

where $(a_i)_n$ and $(b_j)_n$ are Pochhammer symbols which can be respectively defined as

$$ (a_i)_n = (a_i)(a_i+1)(a_i+n-1) = \frac{\Gamma(a_i+n)}{\Gamma(a_i)} \quad (A3) $$

$$ (b_j)_n = (b_j)(b_j+1)(b_j+n-1) = \frac{\Gamma(b_j+n)}{\Gamma(b_j)} \quad (A4) $$

## The notations of crucial specific functions and variables

Since many crucial specific functions and variables have been introduced in this work, a table of their notations will be shown here for the convenience of those unfamiliar readers.

***Table 1:*** *Notations of crucial specific functions and variables.*

| Function/Variable | Notation |
|---|---|
| $C_\alpha$ | Pseudo capacitance |
| Ci() | Cosine integral function |
| $\frac{d^\alpha}{dt^\alpha}$ | $\alpha^{\text{th}}$ order Fractional derivative operator |
| $E_\alpha()$ | Mittag-Leffler function |
| $E_{\alpha,\beta}()$ | Generalized Mittag-Leffler function |
| ${}_p\tilde{F}_q(;\ ,\ ;)$ | Regularized hypergeometric function |
| ${}_pF_q(;\ ,\ ;)$ | Generalized hypergeometric function |
| $t_{c\alpha}$ | Fractional time constant |
| $t_d$ | Delay time |
| $t_r$ | Rise time |
| $t_s$ | Settling time |
| Si() | Sine integral function |
| $t_{PMMA}$ | Thickness of polymethyl methacrylate coating film on the electrode |
| $W$ | Rational power complex variable |
| $\alpha$ | Order of fractional derivative |
| $\Gamma()$ | Gamma function |
| $\sigma$ | Fractional time component |

**Rawid Banchuin** received the B.Eng. degree in electrical engineering from Mahidol University, Bangkok, Thailand in 2000, the degree of M.Eng. in computer engineering and Ph.D. in electrical and computer engineering from King Mongkuts University of Technology Thonburi, Bangkok, Thailand in 2003 and 2008 respectively. At the present, he is an assistant professor of the Graduated School of Information Technology and Faculty of Engineering, Siam University, Bangkok, Thailand. His research interests are computation and mathematics in electrical and electronic engineering especially the fractional order and memristive devices, circuits and systems.

**Roungsan Chaisricharoen** received B.Eng., M.Eng. and Ph.D. degrees from the department of computer engineering, King Mongkuts University of Technology Thonburi, Bangkok, Thailand. He is an assistant professor at the school of information technology, Mae Fah Luang University, Chiang Rai, Thailand. His research interests are computational intelligence, analog circuits and devices, wireless networks and optimization techniques. At the present, Asst. Prof. Dr. Roungsan Chaisricharoen is a member of ECTI board committee, public relations personal of ECTI.